Monte Carlo study of a triangular Ising lattice-gas model with two-body and three-body interactions

Kuan Ken Chin* and D. P. Landau
Center for Simulational Physics, University of Georgia, Athens, Georgia 30602
(Received 6 October 1986)

The behavior of a triangular Ising lattice-gas model with both two- and three-body coupling between nearest neighbors is studied using Monte Carlo methods. The phase diagrams in both field-temperature space and coverage-temperature space are determined for a wide range of interactions and are compared with the predictions obtained using various theoretical approaches.

I. INTRODUCTION

The triangular Ising model with antiferromagnetic nearest-neighbor (NN) coupling has long been of interest because of its highly degenerate ground state and the lack of a transition in zero magnetic field.[1] In the presence of a magnetic field two ferrimagnetic ordered states become stable and are separated from the disordered state by lines of second-order phase transitions.[2,3] It can be easily shown that this model is identical to a lattice-gas model[4] which is useful for the understanding of adsorbed monolayers of rare-gas atoms on graphite.[5,6] In Fig. 1 we show equivalent representations of the ordered $(\sqrt{3}\times\sqrt{3})$ structure in magnetic and in lattice-gas language. This structure may be understood by dividing the lattice into three equivalent next-nearest-neighbor (NNN) sublattices and filling one sublattice with down-spins (occupied sites) and two sublattices with up-spins (empty sites). In zero field this ferrimagnetic spin-up structure is equivalent to a state with all spins reversed to form a ferrimagnetic spin-down state, i.e., a $(\sqrt{3}\times\sqrt{3})^*$ state with $\frac{2}{3}$ of the sites filled and $\frac{1}{3}$ of them empty. In order to understand the behavior of potentially more realistic models, studies have been made including NNN interactions[7–10] or three-body coupling on a NN triangle.[3,11–16] The effect of adding three-body coupling was first studied using mean-field theory by Froyen *et al.*[13] However, since mean-field theory has been inaccurate in its predictions for a number of models with competing interactions,[8,17,18] its predictions for this model must be viewed cautiously. More recent and more sophisticated treatments[3,14,15] are likely to be more reliable. In addition to its application to adsorbed monolayers, the model which includes three-body coupling has also been used to describe lithium intercalation in transition-metal dichalcogenides.[16]

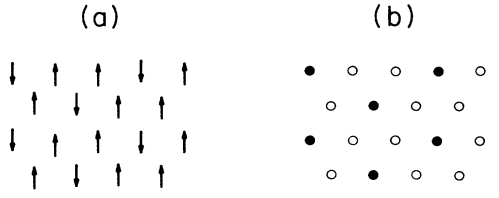

FIG. 1. Equivalent ordered structures: (a) ferrimagnetic structure with net magnetization $+\frac{1}{3}$; (b) lattice-gas structure with $\frac{1}{3}$ of the sites occupied (occupied sites are shown by solid circles).

In this paper we report the results of extensive Monte Carlo studies on the triangular Ising lattice-gas model with nearest-neighbor two-spin and three-spin interactions in the presence of a magnetic field. We shall compare our results with the predictions made by Schick *et al.*[3] using real-space renormalization-group (RG) calculations as well as those obtained using interface[14] and variational methods.[15] Real experiments on magnetic systems are carried out by controlling magnetic field and temperature while experiments on adsorbed monolayers generally involve fixing the coverage (i.e., magnetization). In presenting our results we shall therefore show phase diagrams in both thermodynamic planes. Our intent was to determine phase diagrams for a wide range of interactions; therefore, the data which will be presented are of modest accuracy for each set of couplings. In Sec. II we present background on the model and methods used, and in Sec. III shall present our results.

II. BACKGROUND

A. The model

We have studied the triangular Ising model with two-spin coupling J between nearest-neighbors and three-spin coupling P between sites at the vertices of a NN triangle. A magnetic field H is included and the Hamiltonian is thus:

$$\mathcal{H}_I=-J\sum_{\langle ij\rangle}\sigma_i\sigma_j-P\sum_{\langle ijk\rangle}\sigma_i\sigma_j\sigma_k-H\sum_i\sigma_i\ , \tag{1}$$

where $\sigma_i=\pm1$. The model can be transcribed to an equivalent lattice-gas model involving site occupation variables $c_i=1,0$ with

$$c_i=\tfrac{1}{2}(1-\sigma_i) \tag{2}$$

and NN two-body coupling $\phi_{\rm NN}$ and three-body coupling ϕ_t:

$$\mathcal{H}_{\rm LG}-N_a\mu=-\phi_{\rm NN}\sum_{\langle ij\rangle}c_ic_j-\phi_t\times\sum_{\langle ijk\rangle}c_ic_jc_k-(\epsilon+\mu)\sum_i c_i\ , \tag{3}$$

where N_a is the number of adatoms ($=\sum c_i$), ϵ is binding energy of an adatom, and μ is the chemical potential. (Note that the Ising model in a canonical ensemble is equivalent to the lattice-gas model in the grand canonical ensemble.) The two Hamiltonians are identical if

$$J=\tfrac{1}{4}\phi_{NN}+\tfrac{1}{4}\phi_t \ , \tag{4a}$$

$$P=-\tfrac{1}{8}\phi_t \ , \tag{4b}$$

$$H=\tfrac{1}{2}(\epsilon+\mu)-\tfrac{3}{2}\phi_{NN}-\tfrac{3}{4}\phi_t \ . \tag{4c}$$

From Eq. (2) we see that the coverage n of the lattice-gas model is related to the magnetization M of the Ising model by $n=(1-M)/2$. In addition, certain features of the phase diagrams for this model can be related to the properties of the hard-hexagon model.[19] For example, the high-field low-temperature phase boundary should be linear, i.e.,

$$\frac{k_BT}{|J|}=a\,|H-H_c| \ , \tag{5}$$

where a is related to the critical fugacity of the hard hexagons and has the value $a=0.83$. The corresponding critical density of hard hexagons is $n_c=0.276$ which then yields a critical magnetization of $M_c=0.447$ in the Ising model.

B. Method

We have used a standard, single spin-flip Monte Carlo technique[9] on an IBM 3081 computer to study $L\times L$ triangular lattices with periodic boundary conditions. Most of the data were obtained for $L=36$. A minimum of 250 MCS (Monte Carlo steps per site) were retained for com-

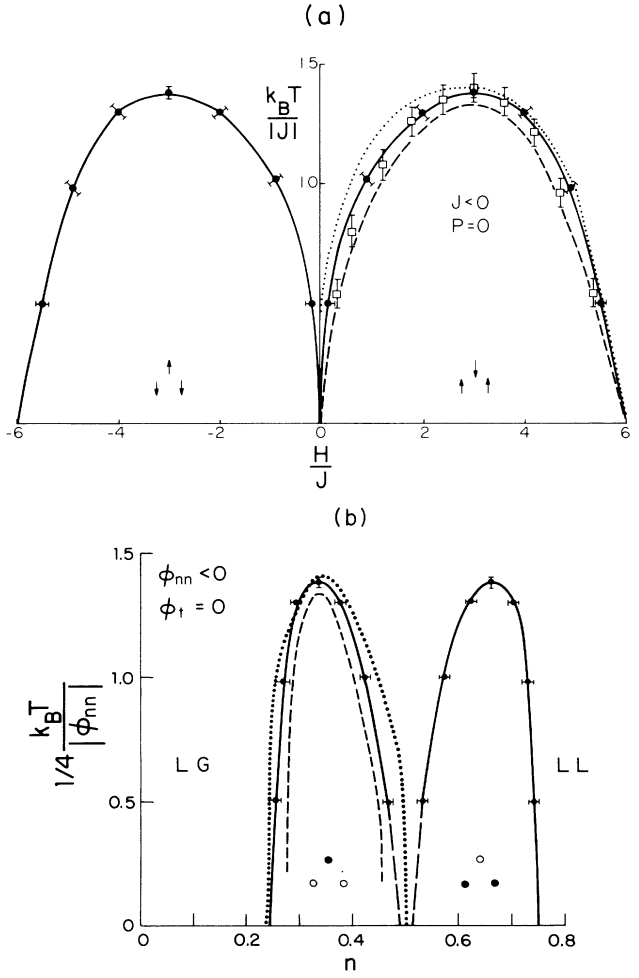

FIG. 2. Phase diagram with only antiferromagnetic two-body coupling. (a) Field-temperature space: RG results (· · ·), transfer-matrix results (— — —), Monte Carlo results of Metcalf (□), and current Monte Carlo data (●). (b) Coverage-temperature space: RG results (· · ·), transfer-matrix result (— — —), and current Monte Carlo results (●). LG and LL refer to lattice-gas and lattice-liquid regions, respectively.

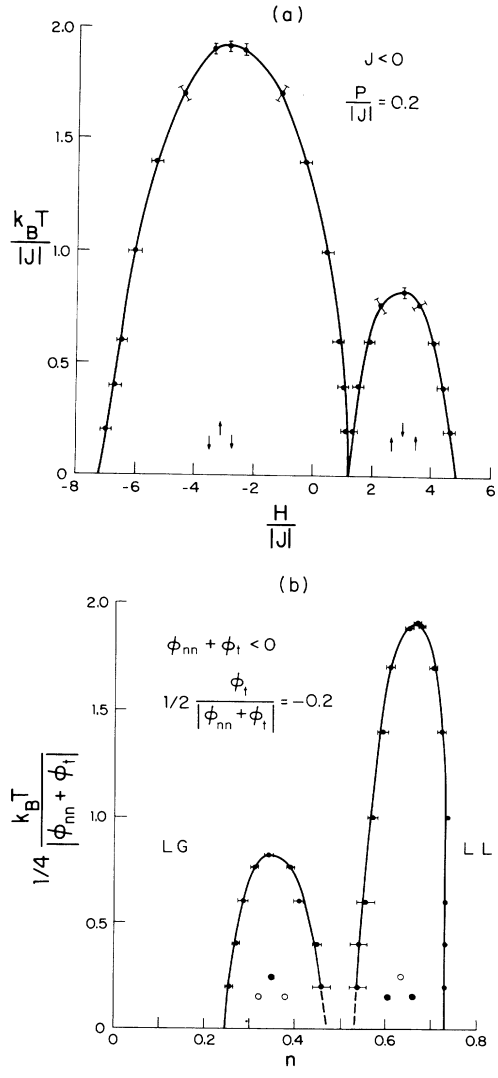

FIG. 3. Phase diagram for $P/|J|=0.2$ with $J<0$: (a) field-temperature space; (b) coverage-temperature space.

puting averages for each data point and near phase transitions as many as 2000 MCS were retained. Data were obtained along paths of constant temperature T, constant field H, or constant H/T; in all cases data were obtained while moving in both directions along the path chosen.

Several of the phase boundaries turned out to be first order and showed pronounced hysteresis. In order to determine the actual location of the phase transition we used a method of free-energy comparison which has proven very successful for the fcc Ising antiferromagnet.[20] The free energy is given by

$$F(T,H)=U(T,H_1)-\int_{H_1}^{H} MdH \tag{6}$$

if H_1 is very large; and for small H_1 we use the usual thermodynamic relation

$$F(T,H)=F(T,H_1)-\int_{H_1}^{H} MdH\ , \tag{7}$$

where $F(T,H_1)$ is determined from internal energy and integration of the low-temperature specific heat. Starting from either side of the hysteresis, we can use Eqs. (6) and (7) to obtain the two branches of the free energy. The intersection of these two branches yields the location of the first-order transition.

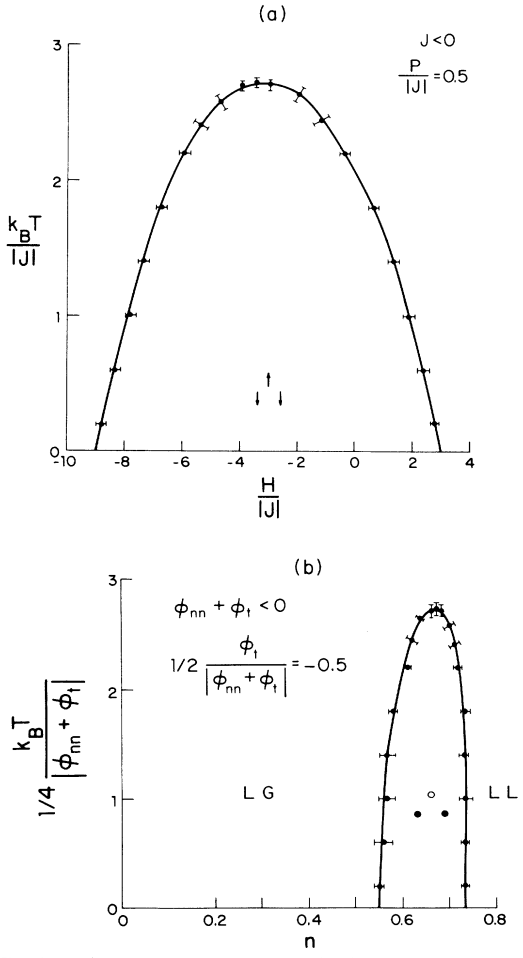

FIG. 4. Phase diagram for $P/|J|=0.5$ with $J<0$: (a) field-temperature space; (b) coverage-temperature space.

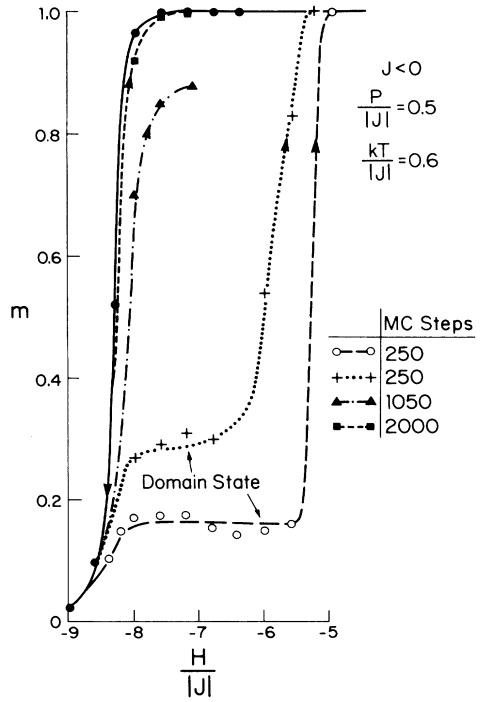

FIG. 5. Apparent hysteresis at a second-order phase transition for $P/|J|=0.5$ with $J<0$. The actual critical field is $H_c/|J|=-8.6$.

III. RESULTS

A. Antiferromagnetic two-spin coupling: $J<0$

1. $P=0$

In the case where there is no three-spin coupling (i.e., $P=0$) the model described by Eq. (1) reverts to the simple triangular Ising antiferromagnet. In Fig. 2(a) we compare our Monte Carlo results for the phase diagram in

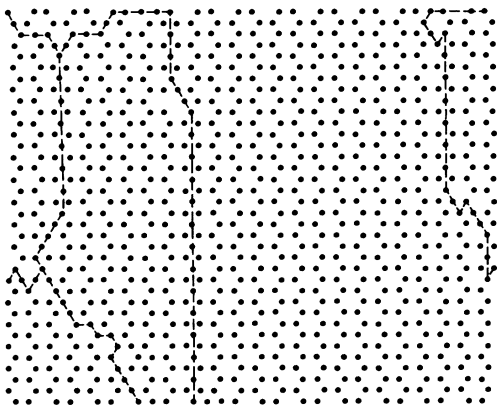

FIG. 6. Domain wall state for $P/|J|=0.5$ with $J<0$. Configuration is for $k_BT/|J|=0.2$, $H/|J|=-8.4$. Dashed lines show centers of domain walls.

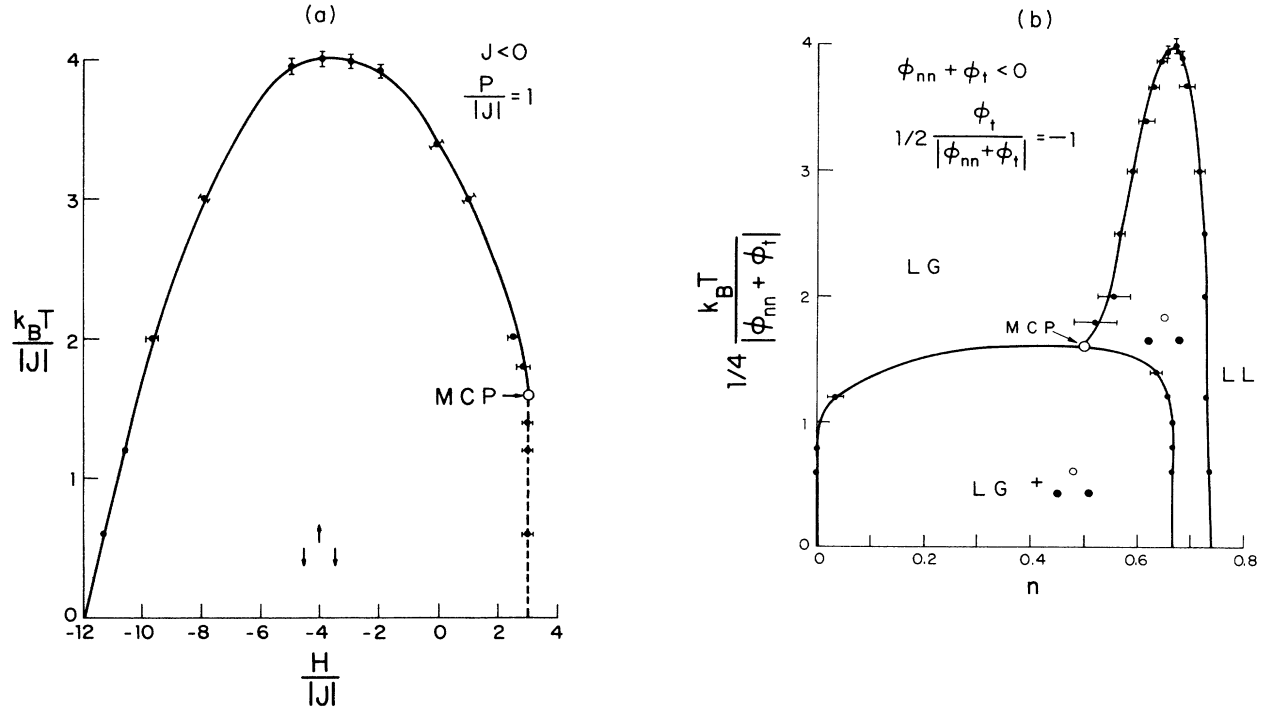

FIG. 7. Phase diagram for $P/|J|=1$ with $J<0$: (a) field-temperature space. First-order phase boundaries are dashed lines and second-order transitions are solid lines; (b) coverage-temperature space.

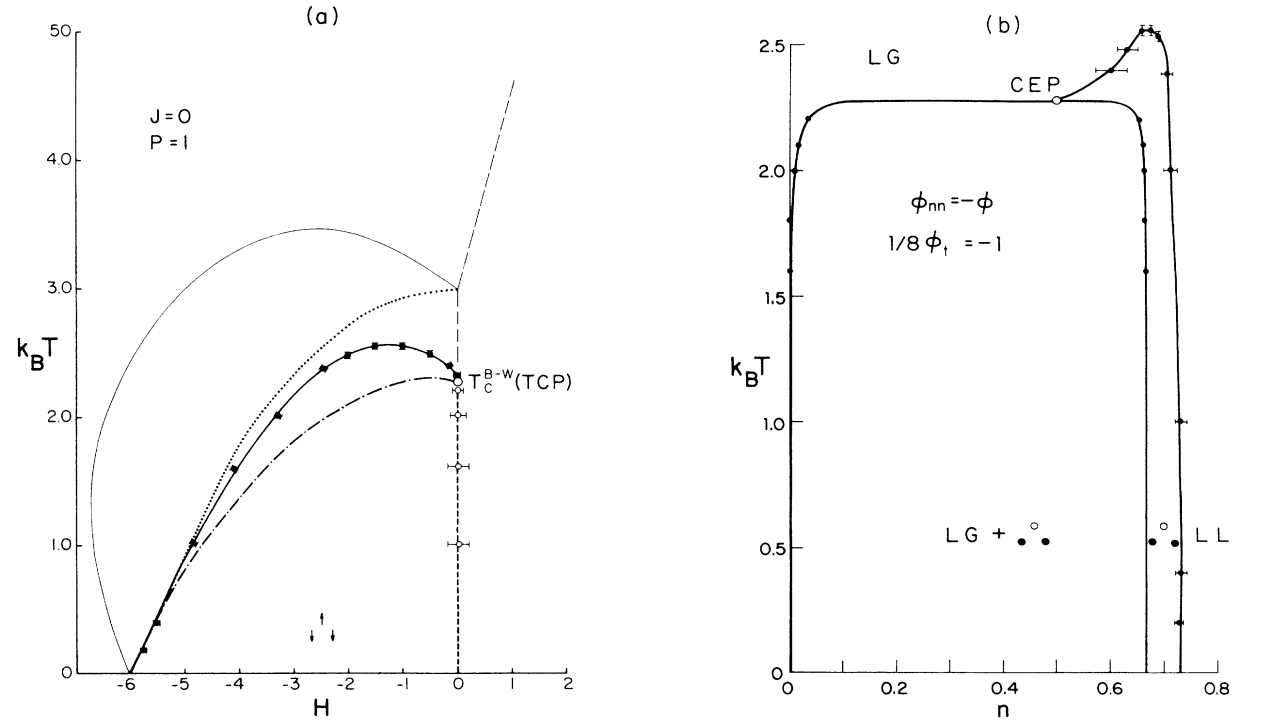

FIG. 8. Phase diagram for the Baxter-Wu model, $J=0$, $P=1$: (a) field-temperature space. The thin solid line shows the result of mean-field theory (Ref. 13), the dotted line gives the interface theory result (Ref. 14), and the dot-dashed line shows the prediction from the variational theory (Ref. 15); (b) coverage-temperature space.

H-T space with those of Metcalf[2] as well as with the real-space RG values of Schick *et al.*[3] and the transfer-matrix result of Kinzel and Schick.[21] (The phase diagram is symmetric about $H=0$; we have showed all results only for $H>0$.) Our estimates, for $L=36$, agree well with those of Metcalf, for $L=99$, for $k_BT/|J| \gtrsim 1.0$. At lower temperatures, although the error bars for the two sets of data overlap, our estimates fall consistently outside of those of Metcalf particularly near $H/|J|=0$. Since our lattices were smaller than those used by Metcalf we expect some of the difference to be due to finite-size effects.[20] Indeed the high field slope of the phase boundary which we obtained was $a=0.96$ [see Eq. (5)] which is substantially higher than the exact value of 0.83 obtained from the critical fugacity of the hard-hexagon model.[22] For small H the behavior of T_c is not inconsistent with the linear approach to zero suggested by Kinzel and Schick[21] and confirmed by Nienhuis *et al.*[23] In Fig. 2(b) we also show the phase diagram in the coverage-temperature plane. Note that the phase diagram is symmetric about $n=0.5$. Our Monte Carlo data lie between the renormalization-group (RG) and transfer-matrix curves but differ noticeably from both. Our estimate of $n_c=0.25$ for the lower critical coverage is slightly below the exact value (obtained from the hard-hexagon results[22]) of $n_c=0.276$. We have not attempted to accurately determine the critical magnetization for $H=0$ but a reasonable extrapolation supports the conclusion of Kinzel and Schick[20] that a gap exists in the critical coverage for the two ordered phases.

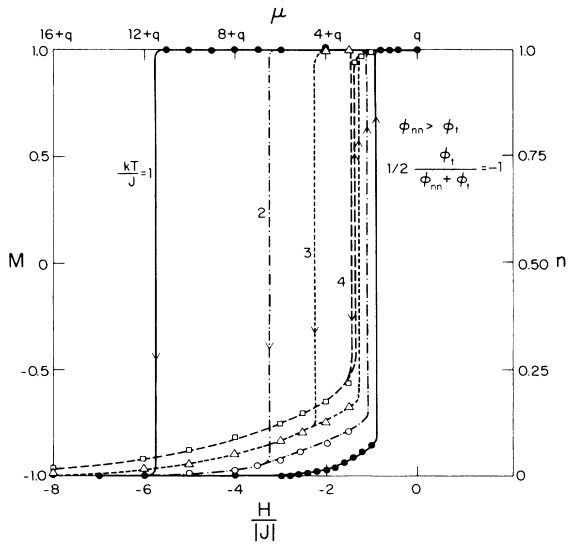

FIG. 9. Hysteresis along isotherms below the critical point for $J>0$, $P/J=1$.

2. $P>0$

With the introduction of positive three-spin coupling the phase diagram becomes asymmetric and the net spin-down ferrimagnetic state grows at the expense of the net spin-down state. (Note that for $P<0$ the net spin-up

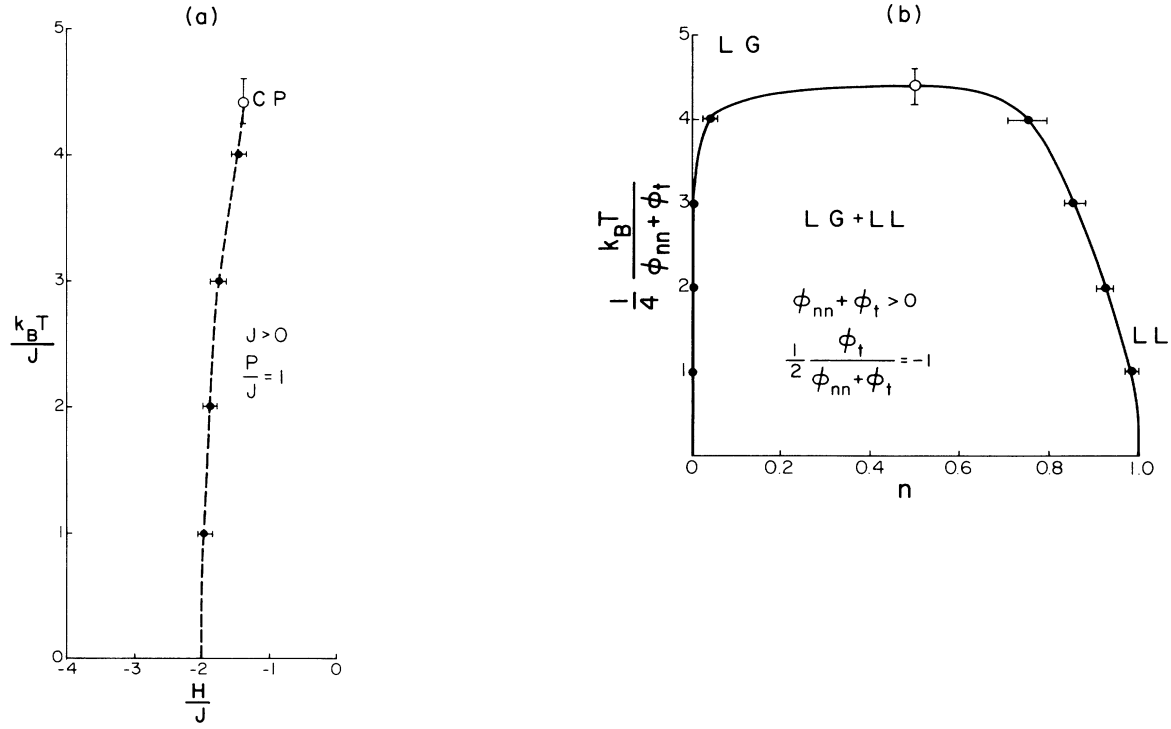

FIG. 10. Phase diagram for $P/J=1.0$ with $J>0$: (a) field-temperature space; (b) coverage-temperature space.

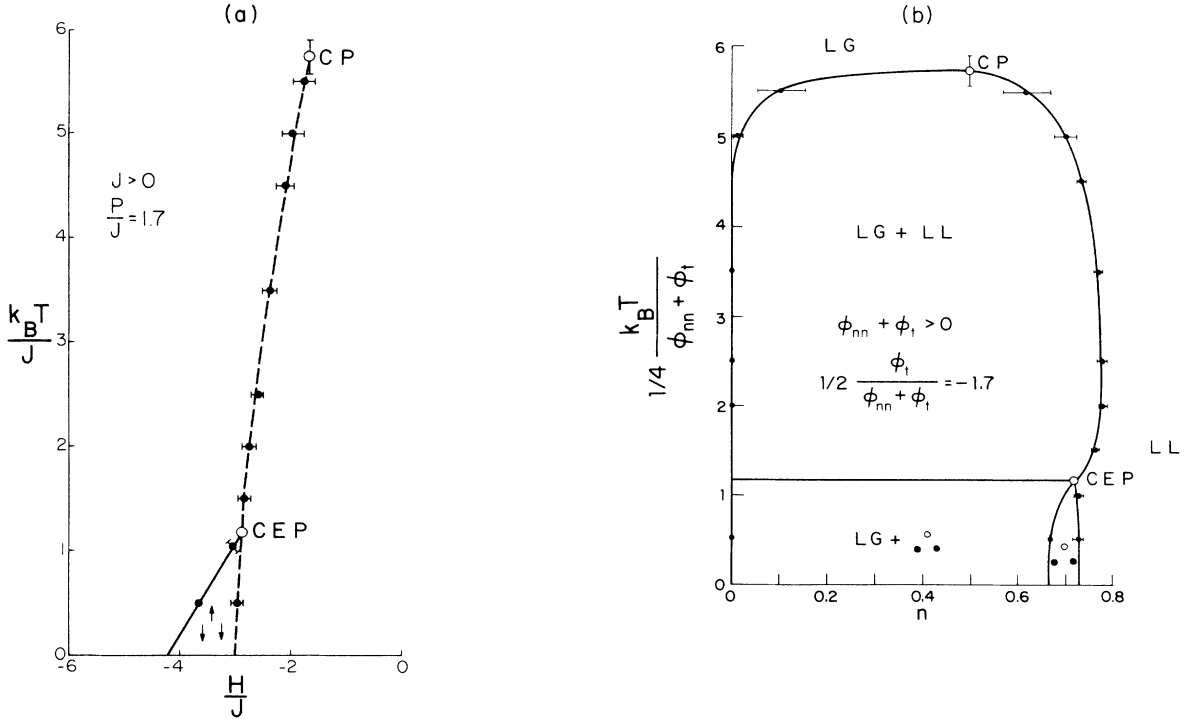

FIG. 11. Phase diagram for $P/J=1.7$, $J>0$: (a) field-temperature space; (b) coverage-temperature space.

state is preferred and the same results are obtained by replacing H by $-H$ and n by $1-n$.) The resultant phase diagrams for $P/|J|=0.2$ are shown in Fig. 3. The asymptotic $T\rightarrow 0$ phase boundaries at large fields are virtually identical: $a_+=0.89$, $a_-=0.90$. In the coverage-temperature plane [Fig. 3(b)] we find that the critical coverages for large fields are quite near to each other in magnitude: $n_c^+=0.73$ ($M_c^+=-0.46$) and $n_c^-=0.25$ ($M_c^-=0.50$). From our results, it also appears that the two ordered phases do not coexist at $n=0.5$ for $T=0$; there appear to be two distinct critical coverages ($n'_+\simeq 0.52$, $n'_-\simeq 0.48$) with a region of disordered phase in between.

By the time $P/|J|=0.5$ the net spin-up state has completely disappeared. The phase boundary in field-temperature space [see Fig. 4(a)] is quite symmetric and the $T\rightarrow 0$ slopes are even the same $a=0.90$. In coverage-temperature space [Fig. 4(b)] a single ordered phase exists in a relatively narrow region. At $T=0$ the critical coverages are $n_c=0.73$ ($M_c=-0.46$) and $n_c'=0.55$ ($M_c'=-0.10$). The low-temperature data at first suggested that the transition might be first order for $H<0$. As shown in Fig. 5 the magnetization showed pronounced hysteresis as the field was swept up and down. Longer runs showed that the apparent hysteresis was due to the formation of metastable domain states. These states, such as that shown in Fig. 6, disappear only slowly due to the relatively slow motion of the domain walls. Note that the domain walls shown in Fig. 6 are not the same walls discussed by Kardar and Berker[24] and by Huse and Fisher[25] in regard to chiral Potts behavior.

The phase diagrams for $P/|J|=1$ are shown in Fig. 7. For $H>0$ the phase boundary is first order and is separated from the second-order boundary by a multicritical point (tricritical point) at $k_BT_t/|J|\sim 1.6$. The low-temperature slope for $H<0$ is $a=0.88$. In coverage-temperature space the first-order transition opens up into a large coexistence region in which the $(\sqrt{3}\times\sqrt{3})^*$ state coexists with the lattice-gas state. At $T=0$ the critical coverage for the pure $(\sqrt{3}\times\sqrt{3})^*$ phase is $n_c=0.74$ and corresponding critical magnetization is $M_c=0.48$.

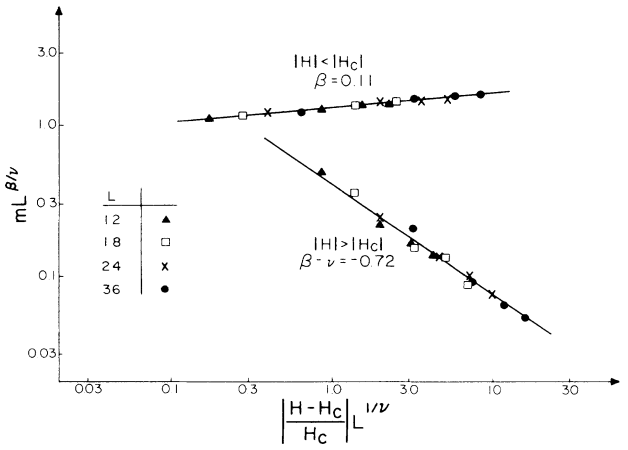

FIG. 12. Critical behavior for $P/J=1.7$, $J>0$ with $k_BT/J=0.5$: finite-size-scaling plot for the order parameter with $\beta=0.11$, $\nu=0.83$.

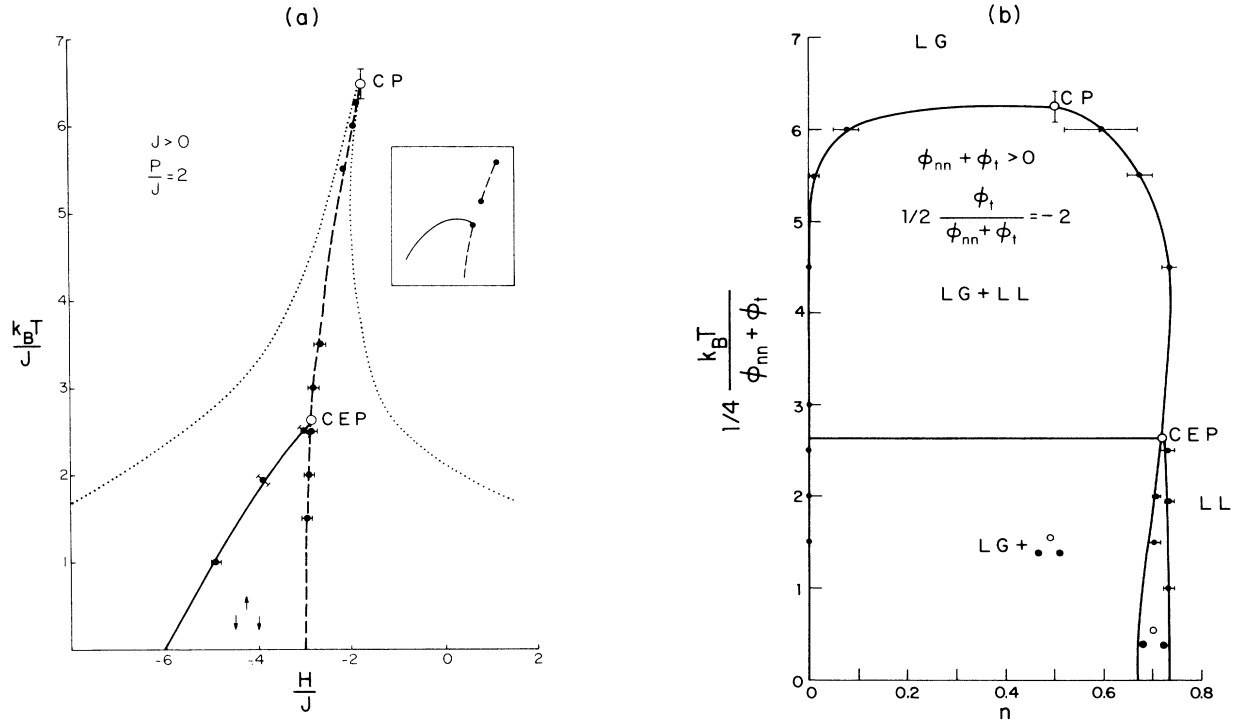

FIG. 13. Phase diagram for $P/J=2$, $J>0$: (a) field-temperature space. The dotted line shows the limits of the hysteresis associated with the first-order transition. The inset shows the RG prediction of Ref. 3. (b) Coverage-temperature space.

B. The Baxter-Wu model: $J=0$

When only three-spin coupling is present this model, known as the Baxter-Wu model,[26] is exactly soluble in zero field with $T_c=2.269$ J/k. The full phase boundary obtained from the Monte Carlo calculations is shown in Fig. 8(a) where it is compared to the predictions of several approximate theories. The mean-field phase boundary is not only quantitatively but also qualitatively incorrect. Although the other theoretical predictions are qualitatively correct, they show noticeable differences with respect to our results and to each other. The low temperature slope of the phase boundary is given by $a=0.88$. A very large coexistence region exists in n-T space [Fig. 8(b)] and the pure ordered phase is confined to a narrow strip with $n_c=0.73$.

C. Ferromagnetic two-spin coupling: $J>0$

For $P=1.0$ we find only a single first-order boundary in the H-T plane terminating in a critical point T_c. The data, shown in Fig. 9, show quite distinct hysteresis below T_c. Both the width and height of the hysteresis loop decrease as T_c is approached and disappear at T_c. The phase diagrams are shown in Fig. 10. In n-T space there is a single coexistence region and no single-phase ordered region.

For $P=1.7$ in addition to a first-order phase boundary we found a small low-temperature pure ordered phase bounded on one side by the first-order transition and on the other side by a second-order phase transition (see Fig. 11). The asymptotic slope a is 0.89. The phase diagram in n-T space is now interesting in that it shows two coexistence regions as well as an ordered phase. Note that $n_c=0.73$ and the single-phase region occupies an extremely small fraction of the overall coverage temperature diagram. We studied the critical behavior for $k_BT/J=0.5$ using finite-size scaling. In Fig. 12 we show a

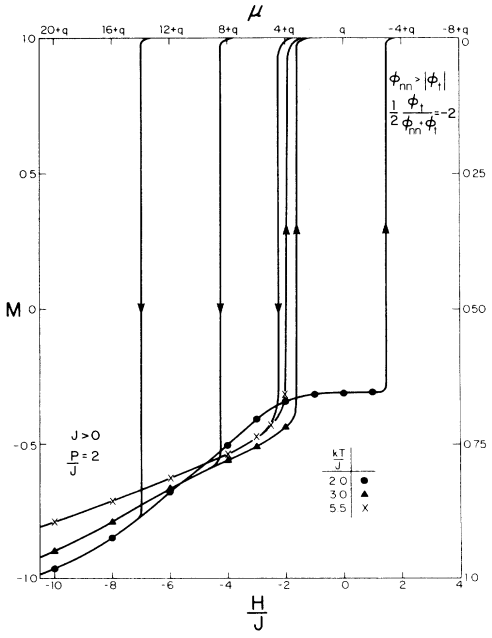

FIG. 14. Hysteresis at the first-order transition for $P/J=2$, $J>0$.

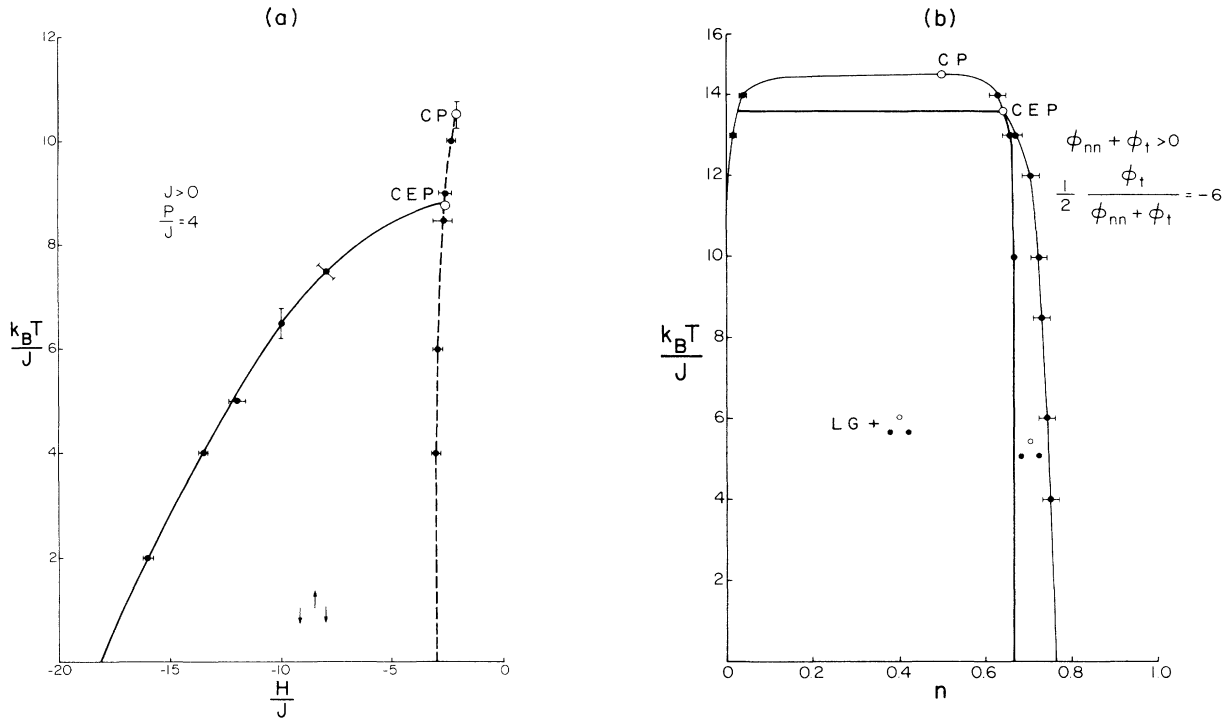

FIG. 15. Phase diagram for $P/J=4$, $J>0$: (a) field-temperature space; (b) coverage-temperature space.

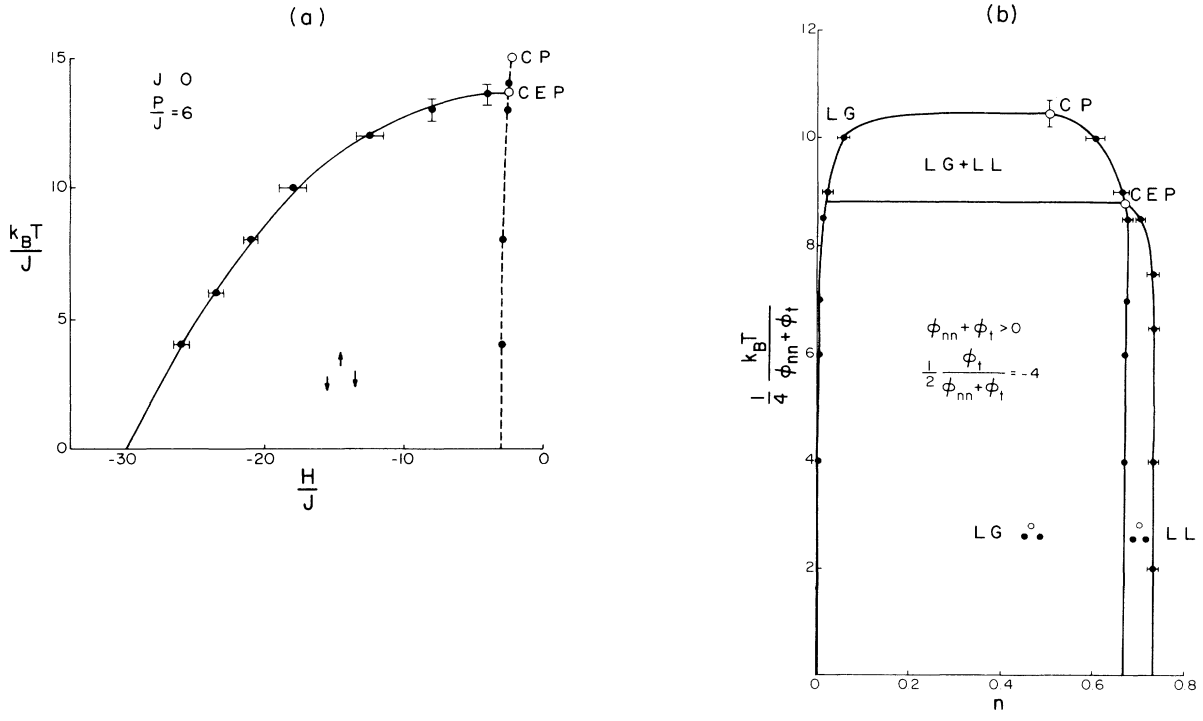

FIG. 16. Phase diagram for $P/J=6$, $J>0$: (a) field-temperature space; (b) coverage-temperature space.

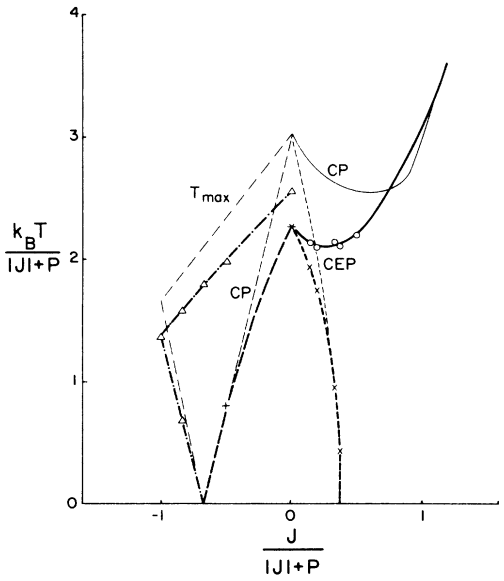

FIG. 17. Dependence of phase-transition points on the three-body coupling. The data points are Monte Carlo results (the heavy curve is a guide to the eye); the thin curves are the theoretical predictions from Ref. 14. (——), Critical point (CP); (— — —), critical endpoint (CEP); (——), tricritical point (TCP); (—·—·), maximum temperature for the $\sqrt{3}\times\sqrt{3}$ phase T_{max}.

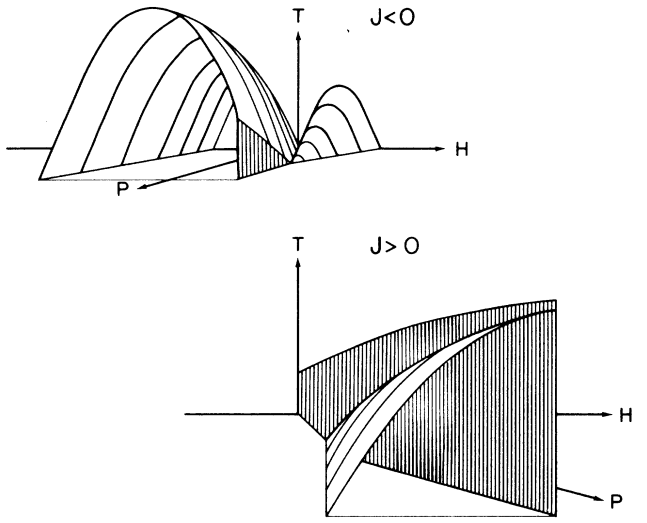

FIG. 18. Schematic phase diagrams in (T,H,P) space. First-order surfaces are shown by closely spaced lines. Second-order surfaces are shown by widely spaced contour lines.

finite-size-scaling plot for the order parameter using $q=3$ Potts exponents. The scatter is random indicating that any deviations from scaling are statistical and not systematic.

The features of the phase diagrams for $P=2.0$, shown in Fig. 13, are qualitatively similar to the previous case. Here we found that the hysteresis was so pronounced (see Fig. 14) that if we swept through the first-order boundary for $T<T_t$ by making the field more negative, we never saw the $(\sqrt{3}\times\sqrt{3})^*$ phase. Hence the locations of both phase boundaries were determined by starting the system in the $(\sqrt{3}\times\sqrt{3})^*$ phase. Note that in this region the RG prediction was that a disconnected first-order region would be found.

For $P=4$ the qualitative features (Fig. 15) are again the same as for $P/J=1.7$ and 2.0. According to RG theory in this region the critical point should occur at the critical endpoint, but our data show that the critical point is clearly higher in temperature. For $P=6$ (Fig. 16) the qualitative trend developed in Figs. 11, 13, and 15 is continued and the critical endpoint and critical point move yet closer together.

In Fig. 17 we plot the dependence of the critical point, critical endpoint, tricritical point, and maximum temperature for the $\sqrt{3}\times\sqrt{3}$ phase on the three-body coupling. The most complete theoretical predictions (Ref. 14), also shown for comparison, are systematically too high in temperature over most of the range of P.

IV. SUMMARY AND CONCLUSION

Using Monte Carlo simulations we have determined the phase diagrams for the triangular Ising lattice-gas model with two-spin and three-spin interactions between nearest neighbors. In Fig. 18 we show a three dimensional (T,H,P) view of the phase diagram; separate representations are shown for $J<0$ and $J>0$. The various phase diagrams which were shown in the previous section are constant P slices of these diagrams. We see that the phase diagrams show qualitative changes due to the addition of the three-body interaction. In some cases the mixed phase regions become substantially larger in coverage-temperature space than the pure phase regions. A comparison with various theoretical approaches shows that none of them properly predict the phase diagrams over the entire range of coupling strengths.

ACKNOWLEDGMENTS

We wish to thank Professors K. Binder and M. Schick for helpful comments. This research was supported in part by National Science Foundation, Grant No. DMR-8603605.

*Present address: Department of Applied Physics, Stanford University Stanford, California 94305.

[1]G. Wannier, Phys. Rev. **79**, 357 (1950); R. M. F. Houtappel, Physica **16**, 425 (1950).

[2]B. D. Metcalf, Phys. Lett. **45A**, 1 (1973).

[3]M. Schick, J. S. Walker, and M. Wortis, Phys. Rev. B **16**, 2205 (1977).

[4]See, M. E. Fisher, Rep. Prog. Phys. **30**, 615 (1967), for both dis-

cussions of this equivalence and references to earlier work on this topic.

[5]The extension of the Ising lattice-gas equivalence to adsorbed monolayers through the addition of an adatom-substrate binding energy was given in G. Doyen, G. Ertl, and M. Plancher, J. Chem. Phys. **62**, 2957 (1975); K. Binder and D. P. Landau, Surf. Sci. **61**, 577 (1976); Phys. Rev. B **21**, 1941 (1980); Surf. Sci. **108**, 503 (1981).

[6]See, e.g., A. N. Berker, S. Ostlund, and F. A. Putnam, Phys. Rev. B **17**, 3650 (1978), and references therein; R. J. Birgeneau, E. M. Hammons, P. Heiney, P. W. Stephens, and P. M. Horn, in *Ordering in Two Dimensions*, edited by S. K. Sinha (Elsevier, New York, 1980).

[7]C. E. Campbell and M. E. Schick, Phys. Rev. A **5**, 1919 (1972).

[8]M. Mekata, J. Phys. Soc. Jpn. **42**, 76 (1977).

[9]D. P. Landau, Phys. Rev. B **27**, 5604 (1983).

[10]B. Mihura and D. P. Landau, Phys. Rev. Lett. **38**, 977 (1977).

[11]H. J. Braathen and P. C. Hemmer, Phys. Norv. **8**, 69 (1975).

[12]D. Imbro and P. C. Hemmer, Phys. Lett. **57A**, 297 (1976).

[13]S. Frøyen, A. A. S. Sudbø, and P. C. Hemmer, Physica **85A**, 399 (1976).

[14]J. Dóczi-Réger and P. C. Hemmer, Physica **109A**, 541 (1981).

[15]A. Malakis, J. Stat. Phys. **27**, 1 (1982).

[16]R. Osório and L. M. Falicov, J. Phys. Chem. Solids **43**, 73 (1982); A. J. Berlinsky, W. G. Unruh, W. R. McKinnon, and R. R. Haering, Solid State Commun. **31**, 135 (1979).

[17]S. Katsura and S. Fujimori, J. Phys. C **7**, 2506 (1974).

[18]D. M. Burley, Proc. Phys. Soc. **85**, 1163 (1965).

[19]This relationship is discussed in Ref. 21.

[20]K. Binder, Z. Phys. B **45**, 61 (1981).

[21]W. Kinzel and M. Schick, Phys. Rev. B **23**, 3435 (1981).

[22]R. J. Baxter, J. Phys. A **13**, L61 (1980).

[23]B. Nienhuis, H. J. Hilhorst, and H. W. J. Blöte, J. Phys. A **17**, 3559 (1984).

[24]M. Kardar and A. N. Berker, Phys. Rev. Lett. **48**, 1552 (1982).

[25]D. Huse and M. E. Fisher, Phys. Rev. Lett. **49**, 793 (1982).

[26]R. J. Baxter and F. Y. Wu, Phys. Rev. Lett. **31**, 1294 (1973); Aust. J. Phys. **27**, 357 (1974).